RESEARCH ARTICLE

Microevolution During Serial Mouse Passage Demonstrates *FRE3* as a Virulence Adaptation Gene in *Cryptococcus neoformans*

Guowu Hu,[a] Shu Hui Chen,[a] Jin Qiu,[a] John E. Bennett,[a] Timothy G. Myers,[b] Peter R. Williamson[a]

Laboratory of Clinical Infectious Diseases, National Institute of Allergy and Infectious Diseases, National Institutes of Health, Bethesda, Maryland, USA[a]; Genomic Technologies Section, Research Technologies Branch, National Institute of Allergy and Infectious Diseases, National Institutes of Health, Bethesda, Maryland, USA[b]

ABSTRACT **Passage in mice of opportunistic pathogens such as *Cryptococcus neoformans* is known to increase virulence, but little is known about the molecular mechanisms involved in virulence adaptation. Serial mouse passage of nine environmental strains of serotype A *C. neoformans* identified two highly adapted virulent strains that showed a 4-fold reduction in time to death after four passages. Transcriptome sequencing expression studies demonstrated increased expression of a *FRE3*-encoded iron reductase in the two strains but not in a control strain that did not demonstrate increased virulence during mouse passage. *FRE3* was shown to express an iron reductase activity and to play a role in iron-dependent growth of *C. neoformans*. Overexpression of *FRE3* in the two original environmental strains increased growth in the macrophage cell line J774.16 and increased virulence. These data demonstrate a role for *FRE3* in the virulence of *C. neoformans* and demonstrate how the increased expression of such a "virulence acquisition gene" during the environment-to-mammal transition, can optimize the virulence of environmental strains in mammalian hosts.**

IMPORTANCE ***Cryptococcus neoformans* is a significant global fungal pathogen that also resides in the environment. Recent studies have suggested that the organism may undergo microevolution in the host. However, little is known about the permitted genetic changes facilitating the adaptation of environmental strains to mammalian hosts. The present studies subjected environmental strains isolated from several metropolitan areas of the United States to serial passages in mice. Transcriptome sequencing expression studies identified the increased expression of an iron reductase gene, *FRE3*, in two strains that adapted in mice to become highly virulent, and overexpression of *FRE3* recapitulated the increased virulence after mouse passage. Iron reductase in yeast is important to iron uptake in a large number of microbial pathogens. These studies demonstrate the capacity of *C. neoformans* to show reproducible changes in the expression levels of small numbers of genes termed "virulence adaptation genes" to effectively increase pathogenicity during the environment-to-mammal transition.**

Received 18 February 2014 **Accepted** 6 March 2014 **Published** 1 April 2014

Citation Hu G, Chen SH, Qiu J, Bennett JE, Myers TG, Williamson PR. 2014. Microevolution during serial mouse passage demonstrates *FRE3* as a virulence adaptation gene in *Cryptococcus neoformans*. mBio 5(2):e00941-14. doi:10.1128/mBio.00941-14.

Editor Gary Huffnagle, University of Michigan Medical School

Address correspondence to Peter R. Williamson, williamsonpr@mail.nih.gov.

Serial-passage experiments with microbial pathogens have demonstrated that strains tend to increase in virulence when passaged in a new host species and lose virulence for the preceding species (1). The fungal pathogen *Cryptococcus neoformans* is an excellent model to study host-dependent mutational changes, as it causes infections in multiple hosts that are chronic, allowing time for significant microevolution. For example, the fungus commonly resides within soil, where it has the capacity to inhabit free-living amoebae (2) and to colonize seedlings of the plant *Arabidopsis thaliana* (3) by using virulence factors such as a polysaccharide capsule and a laccase enzyme for success in each of these host niches, respectively. *C. neoformans* is also a major human pathogen that causes fatal meningoencephalitis in immunocompromised hosts, including those with AIDS, as well as transplant recipients and cancer patients receiving conditioning regimens or chemotherapy, respectively. Worldwide, the fungus accounts for a large proportion of the AIDS-related deaths that occur, reaching 600,000 per year (4), and continues to cause a significant infectious burden in both AIDS and non-AIDS patients in the United States (5).

Mammalian infection is believed to be acquired through the inhalation of yeast cells from the environment into the lungs. Several lines of evidence suggest that the fungus is acquired early in life (6, 7) and may reactivate years later after immune suppression (8). Such long host residence suggests that host adaptation may occur during mammalian residence. Indeed, mouse experiments show increases in the mammalian virulence of *C. neoformans* (9–11), as well as the less virulent species *C. albidus* and *C. laurentii* (12), after serial mouse passage, suggesting that periods of fungal growth in the host may result in microevolution of the pathogen. In addition, extended residence in infected patients has also been associated with phenotypic changes (13, 14). However, the more classical virulence factors laccase and capsule, as well as growth rates *in vitro*, have not shown consistent changes after mouse passage (15) or after passage through nonmammalian hosts such as the amoeba *Dictyostelium discoideum* (16). In contrast, changes in

TABLE 1 Environmental strains used in this study

Isolate	Strain	Origin	Source	Doubling time (h) at 37°C
1	NIH120	Pigeon nest	Chester Emmons, What Cheer, IA	2.7
2	NIH192	Soil	Dexter Howard, Hot Springs, CA	2.9
3	NIH117	Pigeon nest	Chester Emmons, Loudon County, VA	2.8
4	NIH118	Pigeon guano	Chester Emmons, Washington, DC[a]	3.0
5	NIH115	Soil	Chester Emmons, Loudon County, VA	2.5
6	NIH119	Pigeon nest	Chester Emmons, Washington, DC[b]	2.9
7	NIH193	Pigeon cote	Dexter Howard, Westminster, CA	2.6
8	NIH316	Chicken house	Libero Ajello, CDC	3.0
9	NIH404	Soil	Harold Muchmore, Oklahoma	2.8

[a] Junior Village.
[b] Capitol dome.

antifungal susceptibility have been noted (17), as well as modest reductions in capsule size after passage (11), suggesting mutations in unidentified genes. The possibility that such microevolutionary changes may result in clinically relevant increases in virulence is suggested by data showing that cryptococcal isolates successful at disseminating to the brains of solid-organ transplant recipients expressed higher levels of the virulence-associated copper transporter *CTR4* than those limited to causing pulmonary disease (18). However, the genetic mechanisms involved in the optimization of virulence and whether these changes can occur during mammalian residency remain unknown.

More recently, changes in pseudohypha formation between amoeba-adapted and mouse-adapted strains linked to the RAM signal transduction pathway has given insights into the transition between potential restricted ecological niches (19). Free-living amoebae have the ability to act as scavengers for fungi (20–22) and exert pressure for the retention of virulence factors such as the antiphagocytic capsule (2). In the same way, both *C. neoformans* and the related strain *C. gattii* have the ability to act as endophytic fungi, causing either lethal infections or symbiotic colonization in *Arabidopsis* plant seedlings, both dependent on the virulence factor laccase (3). This suggests that genetic and epigenetic changes during the transition between ecologically different environments may provide insight into the acquisition and potentiation of virulence of the fungus.

Thus, to examine physiologically relevant molecular changes during a transition from a soil environment to the mammalian host, we subjected nine serotype A primary culture isolates from soil and pigeon nests to serial passage in mice, followed by recovery from their brains. The expression patterns of two isolates that showed robust increases in virulence after passage were then compared under starvation conditions to identify genes whose expression levels increased after mouse residence. These studies identified an iron reductase gene (*FRE3*) that was significantly upregulated in two strains with increased virulence after mouse passage and remained unchanged in a strain that showed no changes in virulence. The *FRE* family of iron reductases (23) reduce environmental Fe(III) to Fe(II), acting in association with an iron permease (FTR1) and a multicopper ferroxidase Fet3p (24, 25) to facilitate iron uptake in fungi. Iron acquisition during infection is important for infections by diverse bacterial pathogens, as well as fungi such as *C. neoformans* (26). Overexpression of *FRE3* in the two environmental strains facilitated growth in the presence of iron, increased growth rates in macrophages, and recapitulated the increase in virulence in mice after serial passage. These data thus support a relationship between the expression levels of a cryptococcal iron reductase in iron-dependent growth, as well as virulence in *C. neoformans*, during the transition between the environment and a mammalian host.

RESULTS

Serial passage of primary environmental isolates of *C. neoformans* identifies a set of HAVS. A set of nine strains recovered from environmental sources without passage through animals was used for mouse passage studies (Table 1). Classical serotyping was used to identify the strains as serotype A, and genotyping by multilocus sequencing identified the strains as VGI (see Fig. S3 in the supplemental material) as previously described (27, 28). Since passage in laboratory medium is known to result in mutational changes (29), care was taken to minimize laboratory passage. Single colonies of environmental strains were inoculated into Swiss albino mice sequentially four times over a 4-month period, and single colonies were recovered from brains before inoculation into each successive mouse. As shown in Fig. 1A, there was prominent strain-to-strain variability in the acquisition of virulence during mouse passage measured by mouse death (15). Two isolates (no. 6 and 9) showed the most prominent changes, with an approximately 4-fold reduction in the time to death between the first and fourth inoculations (Fig. 1A), and were designated highly adapted virulent strains (HAVS). In contrast, one strain (no. 7) did not change in virulence during the four passages and was selected as a control strain. One of the isolates (no. 1) was unable to achieve sufficient virulence to cause mouse death but did disseminate to the brain in each of the four passages. Comparison of the virulence-associated traits of the nine strains before and after mouse passage found little change in growth rates in yeast extract-peptone-dextrose (YPD) (Fig. 1C) or in capsule size (Fig. 1D). However, changes in laccase expression, measured by determining melanin production, were noted (Fig. 1E) but were not associated with virulence acquisition, except for strain 8, which showed a 2-fold increase in virulence. Fungal survival in the macrophage-like cell line J774.16 (Fig. 1F) showed significant changes in both HAVS, as well as in isolate 4, which showed no change in virulence in mice. In addition, the HAVS were not differentiated from the remainder of the group based on multilocus sequencing (see Fig. S3 in the supplemental material), and all of the strains retained the haploid state after mouse passage (see Fig. S4). In summary, mouse passage of nine environmental strains identified a set of HAVS that showed no consistent changes in the three best-known virulence-associated traits or in genotype-specific similarities.

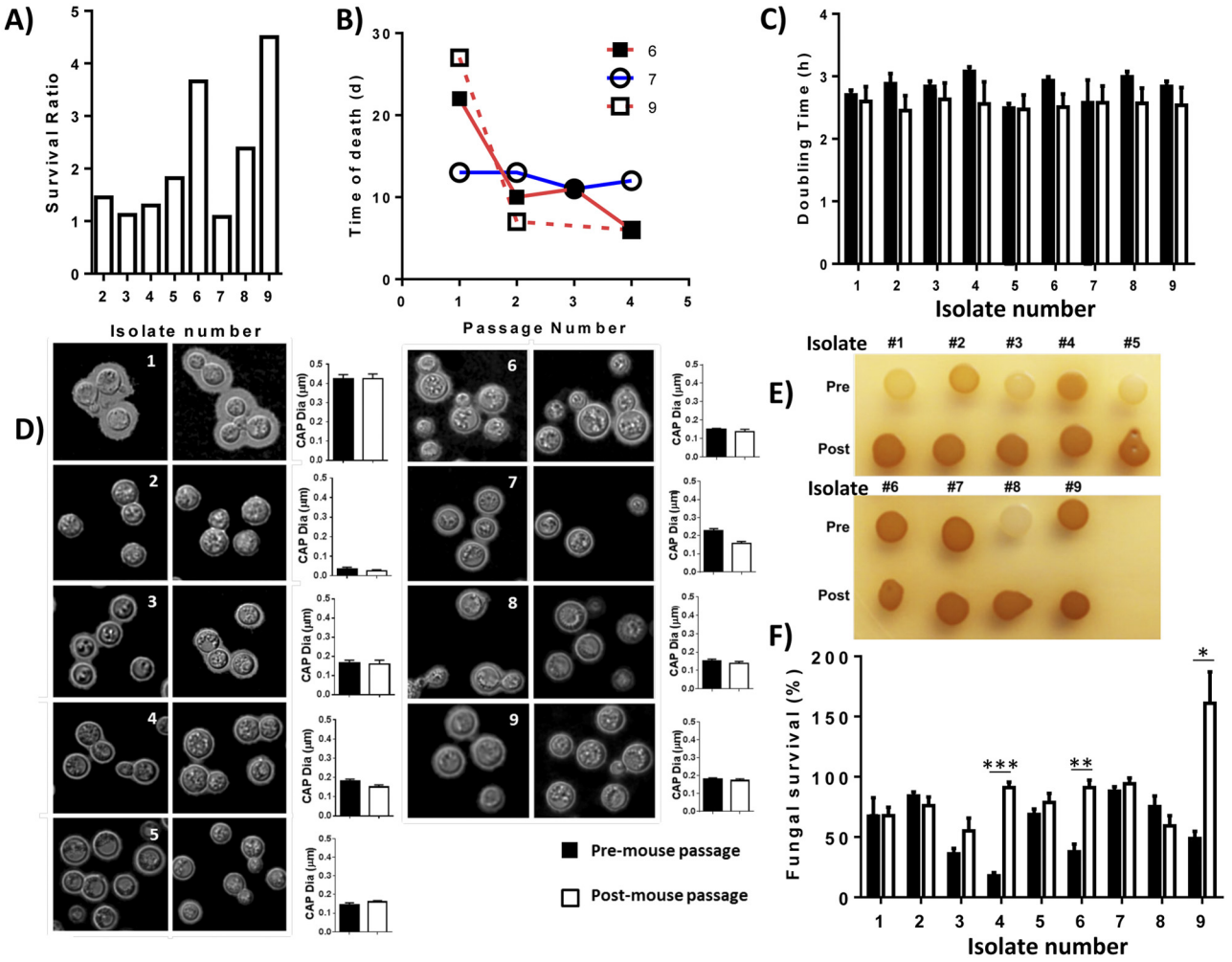

FIG 1 Increased virulence of environmental strains during sequential mouse passages. (A) The environmental isolates indicated (1×10^6 CFU) were inoculated i.v. into Swiss albino mice that were monitored until moribund and then sacrificed. The survival ratio was determined as the ratio of survival time on the first passage versus that on the fourth passage. (B) Time of death versus passage number of the two highly adapted strains (no. 6 and 9) versus a control strain (no. 7) that did not increase in virulence during mouse passage. (C) The strains indicated (1×10^6 CFU) were inoculated i.v. into Swiss albino mice that were monitored until moribund and then sacrificed. (C) Doubling times of the strains indicated prior to (■) and after (□) mouse passage. (D and E) The strains indicated were incubated for 2 days on agar containing 1:10 SAB at 37°C and observed by India ink microscopy for capsule formation (D) or incubated in 0.05% glucose–asparagine salts (pH 7.4) at 37°C for laccase activity determination (E). Pre, prior to mouse passage; Post, after the fourth passage. (F) The strains indicated were subjected to phagocytosis by J774.16 cells, and the fungal CFU counts in aliquots were determined as described in Materials and Methods. Values are means ± SEMs of three independent experiments. *, $P < 0.05$; **, $P < 0.01$; ***, $P < 0.001$.

HAVS demonstrate increased expression levels of an iron reductase after serial mouse passage. To examine whole-genome changes in gene expression associated with increased virulence during mouse passage, the two HAVS isolates, as well as a control strain (no. 7) that did not change in virulence, were compared to their respective environmental predecessor by transcriptome sequencing (RNA-seq). RNA was isolated from fungi under nutrient-depleted conditions, which previously were used to correlate the expression levels of the *CTR4* copper transporter with clinical dissemination to the brains of patients (18). Nutrient depletion also induces a number of virulence-associated traits, such as laccase (30), autophagy (31), and high-affinity glucose transporters (32). Comparison of the expression profiles of two isolates from brains after the fourth passage with those of their respective precursor demonstrated increased transcription (false-discovery rate [FDR], <0.05) >2-fold in four genes in the HAVS (Table 2). In common between the two HAVS was a gene (CNAG_06524) with homology to a set of iron reductase genes of *Saccharomyces cerevisiae*. In addition, HAVS 6 demonstrated increased expression of a predicted protein (CNAG_07853) and HAVS 9 showed increased expression of a conserved hypothetical protein, CNAG_04495. In comparison, control strain 7 showed no significant expression changes in these genes. Real-time quantitative PCR (qPCR) confirmed increased CNAG_06524 expression levels in the HAVS but not the control strain after mouse passage (Fig. 2A). Interestingly, analysis of *FRE3* expression in all nine strains demonstrated a significant increase in expression postpassage in only isolates 6 and 9, with a trend toward increased expression in isolate 8 and little changes in strains that did not increase in virulence (see Fig. S5 in the supplemental material).

The *C. neoformans* genome contains eight putative *FRE*-encoded iron reductases. The CNAG_06524 protein contains

TABLE 2 Genes with >2-fold-increased expression in HAVS versus environmental precursor strains after mouse passage

Locus	Name	Log_2 expression ratio in isolate:			FDR[a]
		6	9	7	
CNAG_06524	Ferric reductase	2.80	2.68	0.43	0.002
CNAG_07853	Predicted protein	2.41	−1.70	−0.50	0.927
CNAG_02691	Conserved hypothetical	2.04	−2.21	0.63	0.831
CNAG_04495	Conserved hypothetical	−0.27	2.94	−0.11	0.039

[a] Adjusted *P* value.

three canonical domains commonly shared by the *FRE* family of iron reductases: a ferric reductase domain and two C-terminal flavin adenine dinucleotide (FAD)- and NADPH-binding domains (33). In addition, using two different predictive programs, seven transmembrane domains were identified, one within the N terminus and six within the ferric reductase domain. Such an organizational structure is typical of the *FRE3* family of proteins from fungi that have no TM domains within the FAD or NAD-binding C-terminal domains (34). Furthermore, a BLAST analysis of CNAG_06524 identified eight putative iron reductases with homology to the *S. cerevisiae* group of eight *FRE3*-encoded iron reductases (Fig. 2C) with closest homology (E = 3e-40; 1e-41) to the Fre2/Fre3 group. Phylogenetic analysis of both Fre protein families clustered both the *S. cerevisiae* Fre2/3 sequence with high support (99%) and the *S. cerevisiae* Fre2-6 sequence with good support (Fig. 2C). Placement of other sequences of both *S. cerevi-*

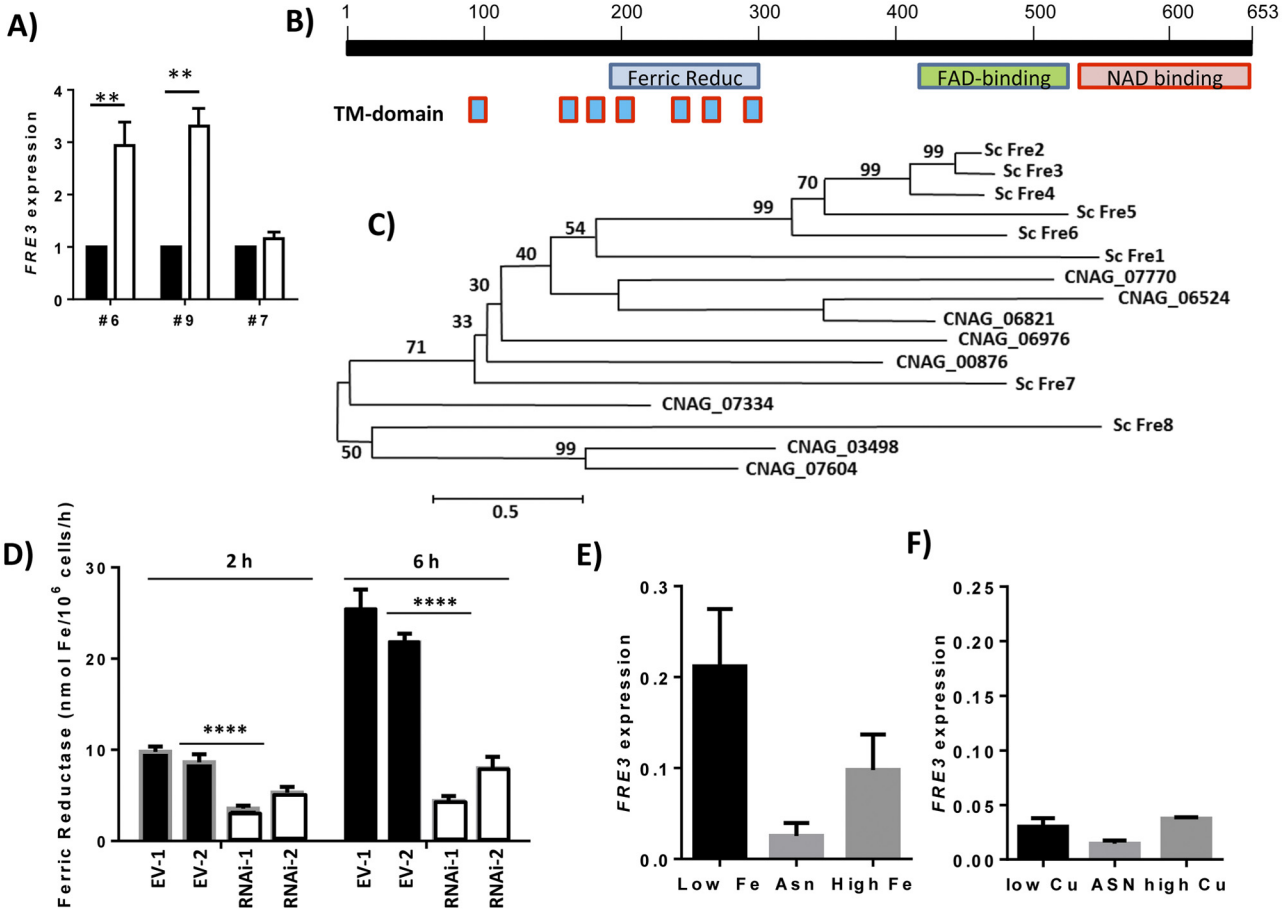

FIG 2 *C. neoformans* FRE3 encodes a cryptococcal iron reductase. (A) *FRE3* expression of the strains indicated. Cells were incubated in ASN medium without glucose for 3 h at 37°C, and *FRE3* transcripts were measured by qPCR as described in Materials and Methods. (B) Scheme of putative protein sequence of the *FRE3* iron reductase (CNAG_06524), including ferric reductase, FAD-binding, NADPH-binding, and transmembrane (TM) domains. (C) ClustalW comparison of *S. cerevisiae* (Sc) and *C. neoformans* (indicated by CNAG number) proteins of the *FRE*-encoded family of proteins. Parsimonious trees were constructed by using the heuristic parsimony algorithm of PAUP 4b10 as described in Materials and Methods. Bootstrap support percentages are shown above branches. (D) Wild-type strain H99 containing RNAi FRE3 suppression plasmids (RNAi-1 and RNAi-2 strains) or the empty vector alone (EV-1 and EV-2) were induced for the times indicated in LIM and monitored by iron reductase assay as described in Materials and Methods. (E) Wild-type H99 cells were incubated in LIM (low Fe), ASN medium (Asn), or LIM after the addition of 2.5 mM $FeCl_3$, and *FRE3* expression was analyzed by qPCR as described in Materials and Methods. (F) Wild-type H99 cells were incubated in low-copper (low Cu) medium, ASN medium, or after the addition of 1.5 mM $CuSO_4$ (high Cu) and analyzed as described for panel E. **, $P < 0.01$; ****, $P < 0.0001$.

siae and *C. neoformans* was problematic, with most bootstrap support values of <70%.

***C. neoformans* Fre3/CNAG_06524 is an iron reductase induced under low-iron conditions without copper reductase activity.** To confirm a role for CNAG_06524 as an iron reductase, two independent RNA interference (RNAi) strains were constructed and iron reductase enzymatic activity was assayed with a fluorophore-coupled assay (35). The reductase activity of two independent transformants (RNAi-1, RNAi-2) was compared to that of two strains containing the empty vector alone (EV-1, EV-2) in equivalent copy number in an H99 genetic background. As shown in Fig. 2D, RNAi suppression of CNAG_06524 resulted in significant suppression of iron reductase activity after induction in low-iron medium for either 2 or 6 h ($P < 0.0001$; $n = 6$). In contrast, a similar assay (35) using copper as the substrate failed to demonstrate significant CNAG_06524-dependent copper reductase activity (data not shown). Transcriptional studies compared expression levels of CNAG_06524 under low- and high-iron conditions and demonstrated elevated expression under low-iron conditions with a minor amount of induction under high-iron conditions that did not reach statistical significance (Fig. 2E). In contrast, induction was not observed with low copper concentrations Fig. 2F, which were tested because the *S. cerevisiae* Fre1 and Fre2 proteins exhibit copper-dependent activities (23, 36). In conclusion, sequence similarity to Fet2 and Fet3, production of an iron reductase activity without copper reductase activity, and induction in low iron but not low copper suggest that CNAG_06524 is most similar to *FRE3* from *S. cerevisiae* (23, 36) and will thus be designated *C. neoformans FRE3*.

Reduced gene dosing of cryptococcal FRE3 results in reduced iron-dependent growth, reduced melanin formation, and reduced survival in macrophages. To assess the role of *C. neoformans FRE3* gene dosing on iron-dependent growth fitness, the growth rates of two independent *FRE3* RNAi strains (RNAi-1, RNAi-2) were compared to those of two equivalent strains expressing the empty plasmid alone (EV-1, EV-2). Since the rates did not differ significantly between the respective RNAi-1 and RNAi-2 strains or between the EV-1 and EV-2 strains, the data were expressed as pooled doubling times (RNAi-1/2, EV-1/2) in three independent experiments with each strain. These studies demonstrated equivalent growth on YPD agar with >90% plasmid retention (data not shown) but reduced growth on low-iron medium (Fig. 3A) (doubling times: RNAi-1/2, 9.3 h; EV-1/2, 16.4 h [$P < 0.0001$]). *FRE3* suppression also reduced growth after moderate iron repletion with 15 μM $FeCl_3$ (Fig. 3B) (doubling times: RNAi-1/2, 3.9 h; EV-1/2, 9.3 h [$P < 0.0001$]) with reduced final concentrations of cells in stationary phase (see Fig. S2 in the supplemental material). A high concentration of iron (2.5 mM) also resulted in reduced growth of the RNAi strains (Fig. 3C) (doubling times: RNAi-1/2, 4.0 h; EV-1/2, 6.6 h [$P < 0.0001$]), although stationary-phase cultures of the two strains reached similar plateau levels (see Fig. S2). In contrast, *FRE3* suppression resulted in minimal suppression of growth in hemin-containing medium (Fig. 3D) (doubling times: RNAi-1/2, 5.7 h; EV-1/2, 7.6 h [$P = 0.05$]), suggesting that *FRE3* has no significant role in siderophore-dependent iron uptake.

FRE3 gene suppression also played a role in virulence factor production and macrophage survival. For example, laccase expression, measured by determining melanin production (Fig. 3E), was dependent on optimal *FRE3* expression, but capsule production on 1:10 Sabouraud medium was not affected (Fig. 3F). However, survival in the macrophage-like cell line J774.16 was attenuated after *FRE3* suppression (Fig. 3G) ($P < 0.01$) suggesting a role in this important phenotype.

Overexpression of *FRE3* in the HAVS precursor strains recapitulates the increased virulence induced by serial mouse passage. To confirm a role for increased *FRE3* expression in adaptive virulence after serial mouse passages, *FRE3* was overexpressed in the HAVS precursors (no. 6 and 9) under the control of an actin promoter. In both strains, overexpression (6-fold overexpression, strain 6-OEx; 9-fold overexpression, strain 9-OEx) resulted in higher growth rates in low-iron medium than of the equivalent strains (6-EV, 9-EV) expressing the empty vector alone (Fig. 4A and B) (doubling times: 6-OEx, 7.7 h; 6-EV, 9.6 h [$P < 0.001$]; 9-OEx, 7.1 h; 9-EV: 10.6 h [$P < 0.001$]). Overexpression also resulted in significantly higher growth rates in medium supplemented with 15 μM $FeCl_3$ (Fig. 4C and D) (doubling times: 6-OEx, 5.1 h; 6-EV, 6.5 h [$P < 0.001$]; 9-OEx, 7.1 h; 9-EV: 9.2 h [$P < 0.05$]). These data suggest that growth in the environmental precursor strains could be further optimized by increasing the expression of the *FRE3* gene. Interestingly, the expression of the two principal virulence factors capsule and laccase was not altered in the two *FRE3*-overexpressing strains (Fig. 4E and F), suggesting that *FRE3* does not alter virulence by increasing these virulence factors. However, overexpression did result in increased fungal survival in the macrophage-like J774.16 cell line, which was statistically significant ($P < 0.01$), an important virulence attribute of this facultative intracellular pathogen (37). Finally, the HAVS precursors overexpressing *FRE3* were inoculated into mice and demonstrated an increase in virulence over strains expressing the empty vector alone (Fig. 4H and I), partially recapitulating the increased virulence induced by mouse passage.

DISCUSSION

Epidemiological (8), as well as serologic (7), work suggests that acquisition of the fungal pathogen *C. neoformans* often occurs early in life and is followed by a latent stage and reactivation prior to the onset of disease, which is akin to diseases such as tuberculosis. This suggests that segments of the human population may harbor the organism and remain susceptible after immune suppression either because of infectious causes as in HIV/AIDS or immunomodulating therapy during transplant conditioning or after cancer chemotherapy. Such a prolonged residence in the mammalian host also suggests a potential to undergo microevolution during mammalian carriage, optimizing pathogenic potential. This optimization occurs on top of an already formidable armamentarium of mammalian virulence factors such as an antiphagocytic capsule, potentiated in ecological niches containing free-living amoebae (2), or an immunomodulatory factor such as laccase, required for colonization and infection of seedling plants (3). Thus, the present study sought to identify genes that have the capacity to both (i) facilitate virulence and (ii) undergo permitted transcriptional inductions during the environment-to-mammal transition. Interestingly, after four passages through mice, the environmental strains showed a markedly different propensity to increase virulence, with two HAVS reducing the time to death by a factor of four, whereas the other strains showed little or no difference in virulence; indeed, one strain remained unable to kill mice after 60 days despite successful brain infection. This variation in the acquisition of virulence in unrelated strains has been

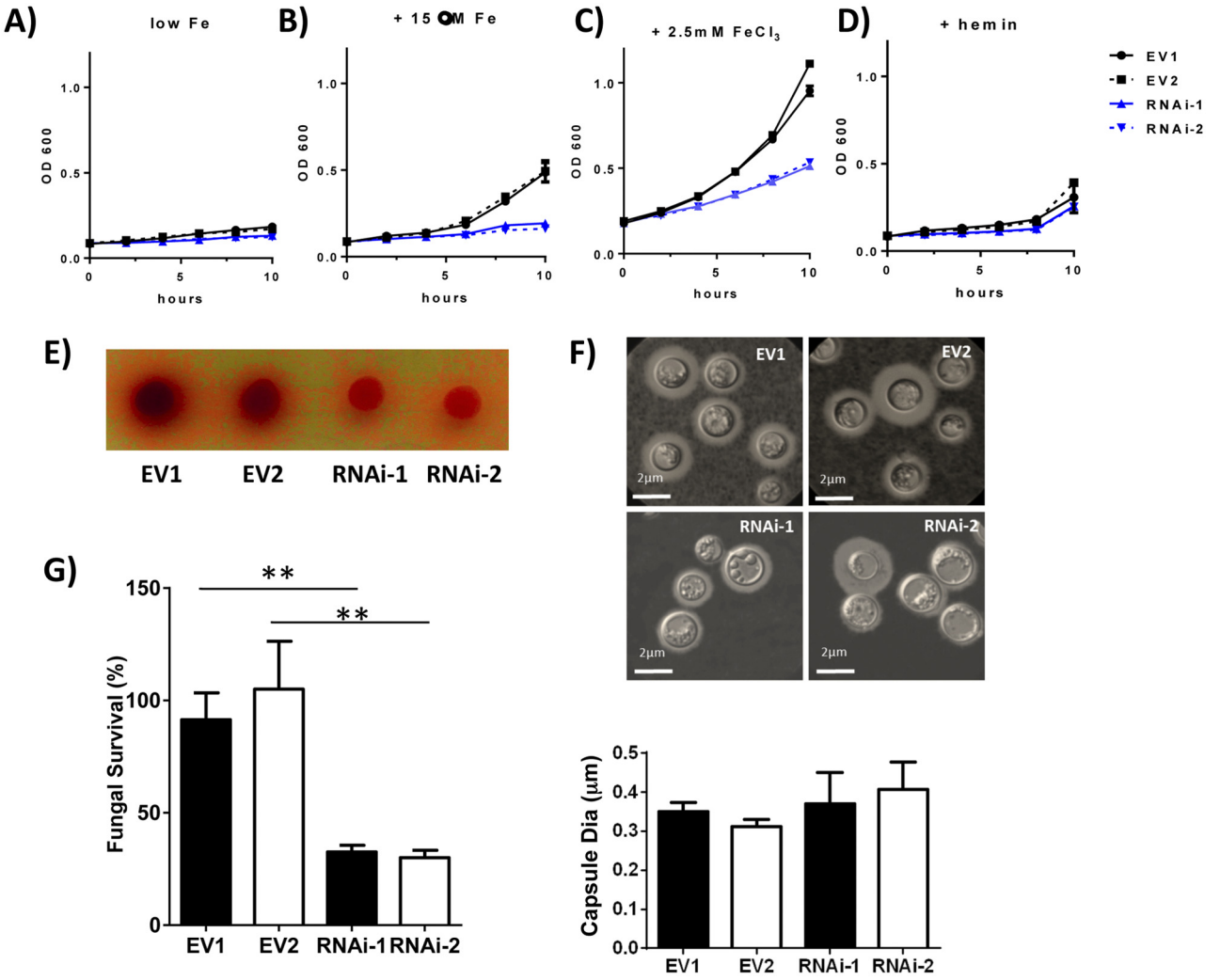

FIG 3 *C. neoformans* FRE3 suppression in a virulent H99 strain suppresses growth, laccase activity, and fungal survival in a macrophage-like cell line. (A to D) *FRE3* suppression strains in an H99 background (RNAi-1, RNAi-2) and empty-vector controls (EV1, EV2) were grown in the media indicated and monitored for growth by measurement of optical density at 600 nm (OD 600). (E) The laccase activities of the strains indicated were assayed by measuring melanin formation. (F) Capsule was induced by growth on 1:10 SAB medium, and capsule size was observed (top) and measured (bottom) by differential interference contrast microscopy. (G) Fungal survival of the strains indicated in J774.16 cells was assessed by counting fungal CFU and expressed as a percentage of the input after the removal of phagocytosed and adherent cells by washing as described in Materials and Methods. Results of three independent experiments are shown. **, $P < 0.01$.

reported previously and is likely due to genetic background differences (11, 38).

With this experimental environment-to-mammal transition model, a whole-genome approach identified increases in the transcription of a cryptococcal *FRE3*-encoded iron reductase not previously identified as having a role in fungal virulence. This whole-genome search was prompted by previous studies showing a lack of correlation of known virulence factors with virulence acquisition in mice (11) and was confirmed in the present studies. The best-studied family of *FRE3*-encoded iron reductases is that of the model yeast *S. cerevisiae*, which, like that of *C. neoformans*, contains eight members (23). Iron acquisition requires an elaborate mechanism for acquisition by fungi because the metal is water insoluble and is maintained in the metabolically inactive ferric form Fe(III) because of the presence of dissolved oxygen (39). Iron reductases contain three canonical domains, a heme-containing six-transmembrane ferric reductase domain and two C-terminal cytoplasmic FAD- and NADPH-binding domains (33), which act together in two half reactions whereby reduction of Fe(III) to Fe(II) is coupled to the oxidation of dioxygen to superoxide radical (33). Reduced iron is then acquired by copper-containing Fet3, which then oxidizes iron back to Fe(III) as it is transported across the cell wall in concert with an *FTR1*-encoded iron permease (40). These domains are present in homologous proteins from other fungal pathogens such as *Paracoccidioides brasiliensis* (41). Linkage of the iron acquisition machinery with that of copper is suggested by a requirement of Fet3 for its copper cofactor (42). Not surprisingly, this linkage extends to the iron reductase family, where the *FRE1*- and *FRE2*-encoded proteins are involved in the reduction of both ferric and cupric ions (43). However, in the present study, while the cryptococcal reductase showed the highest homology to the Fre2 and Fre3 proteins, lack of transcriptional dependence on either copper or copper reductase activity led us to designate the cryptococcal protein Fre3,

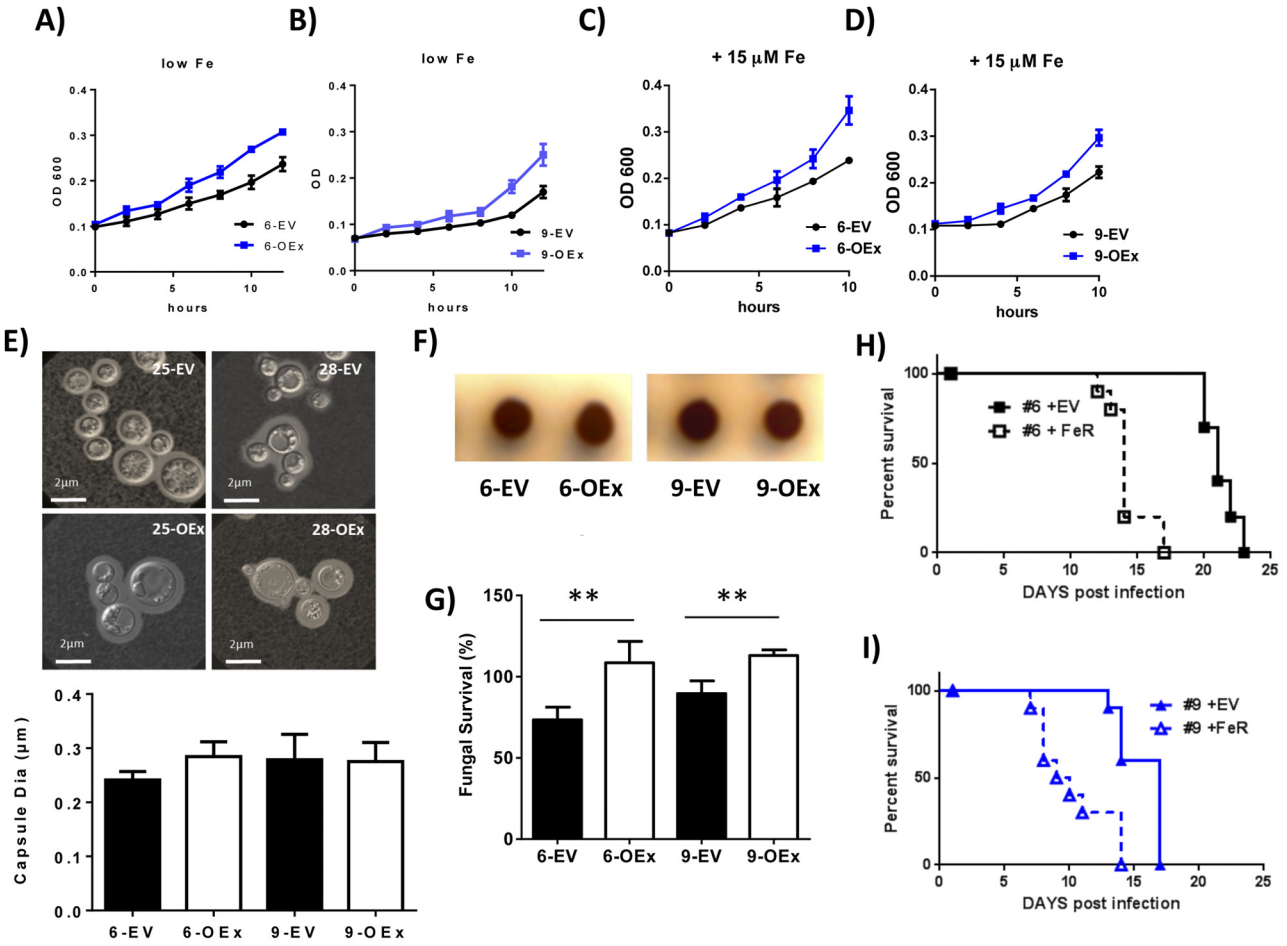

FIG 4 *C. neoformans* FRE3 overexpression in precursor environmental strains increases iron-dependent growth, survival in macrophages, and virulence in a mouse model. (A to D) *FRE3* was overexpressed in two environmental strains (6-OEx, 9-OEx), and growth in LIM (low Fe) or after supplementation in 15 mM $FeCl_3$ (+ 15 μM Fe) was compared to that of equivalent control strains containing the empty vector (6-EV, 9-EV). (E) Capsule formation was induced by growth on 1:10 SAB medium, and capsule formation was observed (top) and capsule size was measured (bottom) by differential interference contrast microscopy. (F) The laccase activities of the strains indicated were assayed by measuring melanin formation. (G) Survival of the fungal strains indicated in J774.16 cells was assessed by counting CFU and expressed as percent survival after the removal of phagocytosed and adherent cells by washing as described in Materials and Methods. Results of five independent experiments are shown. **, $P < 0.01$. (H, I) The fungal strains indicated (1×10^6 CFU) were inoculated i.v. into Swiss albino mice, which were sacrificed when moribund.

which is more exclusively an iron-regulated and iron-reductive protein (23, 36). However, phylogenetic relationships between the *FRE* family in the present studies suggested large differences between the Fre protein sequences of the ascomycete *S. cerevisiae* and the basidiomycete *C. neoformans*, so such a designation can only be approximate at best. *C. neoformans* Fre3p maintained the transmembrane structural signature of fungi (34), suggesting retention of yeast-like iron acquisition requirements for this protein, unlike other *C. neoformans* proteins such as Sp1, which have acquired mammalian features (44). Phenotypically, *FRE3* suppression by RNAi caused reduced growth rates in medium containing $FeCl_3$, which requires reductive iron uptake in *C. neoformans* (45), but without such a defect in the presence of the siderophore hemin, suggesting that *FRE3* has no role in siderophore-dependent growth. *FRE3* RNAi was used in these phenotypic studies rather than knockout strains to simulate the more subtle changes in gene dosing during environment-to-mammal transitions. Knockout strains would be expected to have a more robust phenotype but are less relevant to issues of physiologically relevant phenotypes, as gene deletion per se would be unlikely in wild-type strains. Interestingly, *FRE3* suppression in H99 resulted in reduced laccase activity although *FRE3* overexpression in the environmental strains, either after mouse passage or genetically induced by plasmid-mediated *FRE3* overexpression, did not alter laccase activity, suggesting a threshold effect of *FRE3* gene dosing on laccase activity. Previous studies have noted that iron significantly modulates laccase activity (46) and the *CIR1* iron regulator modulates laccase activity (47). Relationships between iron signaling and laccase may be due to the enzyme's role as an iron oxidase, which has the ability to reduce fungicidal Fenton oxidative products such as hydroxyl radical, produced by macrophages after fungal cell engulfment (48). Interestingly, fungal survival in the macrophage-like cell line J774.16 was also reduced after *FRE3* suppression. Fungal survival is an important attribute of this facultative intracellular pathogen (37) and has been reported to correlate with virulence in cryptococcal strains

such as those of the *C. gattii* outbreak in the Pacific Northwest (49).

To further validate the role of *FRE3* in acquisition of virulence in the HAVS isolates, the environmental precursors were transformed with *FRE3*-expressing plasmids under the control of the *ACT1* constitutive promoter, to simulate the increased expression of the gene after mouse passage. These studies showed that the two environmental strains that had acquired increased *FRE3* expression during mouse passage also developed better iron-dependent growth, better survival in the J774.16 macrophage-cell line, and increased virulence in a mouse model. These results identify *FRE3* as not only a new virulence-associated gene but also as one that is permitted to undergo mammal-restricted transcriptional changes during the transition between the saprophytic and infective states. To clarify this dynamic relationship between the acquisition of virulence and the environment-to-mammal transition, we have used the term "virulence adaptation genes" for genes such as cryptococcal *FRE3*. During the simulated environment-to-mammal transition in the present studies, increased transcription of virulence adaptation genes such as *FRE3* within the mammalian host likely leads to positive selection and increased virulence. These selective pressures led to preferential recovery of HAVS isolates with elevated *FRE3* transcription after mouse passage in two independent environmental strains originally obtained thousands of miles apart from each other. The small number of genes showing transcriptional changes suggests that mouse passage was genetically restricted under these conditions and suggests a model for a genetic "bottleneck" typical of those described where only small numbers of clones survive evolutionary pressures, such as *M. tuberculosis* (50). It also suggests how small changes in expression can increase the virulence of *C. neoformans*, especially considering the wide dissemination of the organism in crowded metropolitan areas, highlighted by isolate 6 from the U.S. Capitol dome in Washington, DC. Interestingly, *FRE3* has not been identified as an upregulated gene in macrophages in previous studies (51), although more recent studies did demonstrate upregulation of iron uptake genes such as the *CFO1*-encoded ferroxidase from "*in situ*" human cerebrospinal fluid samples (52). However, it is important to note that the present study design differs from those used previously in that transcriptional differences between strains were sought (postpassage versus prepassage) rather than differences between conditions (glucose-rich medium versus macrophage environment). Indeed, even a constitutively expressed gene could acquire an increased capacity for expression during mouse passage and increase the overall virulence of a pathogen. However, several caveats apply to the present studies. For example, only a small number of environmental isolates were analyzed after passage; it is expected that additional cryptococcal virulence adaptation genes will be identified by using additional animal models and cryptococcal strains. Other models of infection (pulmonary, for example) offer an environment quite different from that of an intravenous (i.v.) infection and could provide selective pressures to uncover other virulence adaptation genes. However, it is important to use actual environmental strains with limited laboratory passage in such experiments, as the underlying genetic background may affect the mutational mechanism(s) active during these transitions. Additional genes may have been identified by relaxing our stringent criteria of a 2-fold or greater expression change during mouse passage, possibly expanding the scope of biological interpretation. In addition, a role for compensatory mutations that could augment or diminish the effect of *FRE3* mutations was not examined that could influence the true "virulence composite" of the pathogen. Despite these caveats, these studies represent an initial exploration of the environment-to-mammal transition by the whole-genome approach, identifying the potential role of the *FRE3* iron reductase in this important transition.

MATERIALS AND METHODS

Fungal strains, plasmids, and growth media. The *C. neoformans* ATCC 208821 (H99) strain was a gift from J. Perfect, and H99FOA19 was the recipient strain for the expression of green fluorescent protein fusions, overexpression, and RNAi constructs. Environmental strains were obtained from lyophilized cultures in our collection, identified by biochemical reactions (53) and brown-colored colonies on *Guizotia abyssinica* agar, and typed by using serotype-specific absorbed rabbit serum (27). The *URA5* gene was contained in pCIP3 (54) and was the generous gift of J. Edman. Strains were grown in YPD (2% glucose, 1% yeast extract, 2% Bacto peptone), on YPD agar, or in asparagine salts with 2% glucose, 1 g/liter asparagine, 10 mM sodium phosphate (pH 6.5), and 0.25 g/liter $MgSO_4$. Low-iron medium was prepared as previously described (35) and contained, per liter, 20 g of glucose, 5 g of asparagine, 400 mg of K_2HPO_4, 100 mg of $MgSO_4 \cdot 7H_2O$, 50 mg of $CaCl_2 \cdot 2H_2O$, 1 mg of thiamine, 57 mg of boric acid, 396 mg of $CuSO_4 \cdot 5H_2O$, 72 mg of $MnCl_2 \cdot 4H_2O$, 4.2 mg of $ZnCl_2$, and 37 mg of $(NH_4)\,6Mo_7O_{24} \cdot 4H_2O$, buffered with 50 mM 2-(*N*-morpholino)ethanesulfonic acid–NaOH to pH 6.0 and was depleted of iron with Chelex 100 (Sigma) prior to the addition of transition metal salts as previously described (55). Iron supplemented with iron or hemin was prepared by the addition of the indicated amount of $FeCl_3$ or hemin (Sigma).

Virulence factor expression and mouse passage and virulence studies. Capsule formation was assessed on a 1:10 dilution of Sabouraud medium (1:10 SAB) as previously described (56), and the method of Liu et al. (48) was used to measure laccase activity. All experimental procedures were conducted under a protocol approved by the Institutional Animal Care and Use Committee of the Intramural Research Program of the NIAID, NIH. For the i.v. infection model, sets of 6- to 8-week-old Swiss albino mice (Harlan) were infected by tail vein injection of 10^6 CFU of the strains of *C. neoformans* and mutants indicated. For mouse passage experiments, mice were infected as described above, and after sacrifice, two strains were recovered from their brains and grown on YPD agar. The mice were fed *ad libitum* and monitored by inspection twice daily. Mice were euthanized when moribund. Statistical significance of differences in mouse survival times was assessed by Kruskal-Wallis statistics (analysis of variance [ANOVA] on ranks). Statistical analysis was conducted with GraphPad Prism software, version 4.03.

RNA-seq gene expression analysis. Replicate RNA samples were obtained from two strains isolated from the brains of mice after the final environmental passage. The cells were grown to mid-log phase and subjected to starvation at 37°C in asparagine salts (ASN) without glucose for 3 h as previously described (18). RNA was isolated and processed in two independent processing runs, with all six strains represented in each run, i.e., two virulent strains, one nonvirulent strain, and their environmental predecessors. The RNA integrity numbers determined with an Agilent Bioanalyzer were greater than 9.8 for all samples. Sequencing libraries were prepared with Illumina TruSeq RNA Sample Preparation version 1 for the first sample set and version 2 for the duplicate sample set. High-throughput sequencing by synthesis was performed with an Illumina HiScan-SQ with a 100-base paired-end protocol. Approximately 10 million raw reads per library were quality filtered and mapped with BowTie, keeping only those mapped uniquely to the reference sequences from the *C. neoformans var. grubii* H99 Sequencing Project, Broad Institute of Harvard and MIT (http://www.broadinstitute.org/). Transcript abundance values (reads per kilobase per million) were analyzed by lowess normalization of log ratios (after passage/before passage), followed by ANOVA to test for statistically significant expression differences. Reported *P* values

were subjected to Benjamini-Hochberg FDR adjustment for multiple testing.

qRT-PCR experiments. *C. neoformans* strains were grown to the mid-log phase prior to induction by incubation for 3 h at 37°C in asparagine salts as previously described (18). RNA was extracted before and following induction and treated with the RNase-Free DNase Set (Qiagen). Five-microgram samples of total RNA were used for cDNA generation with Invitrogen SuperScript II reverse transcriptase and oligo(dT) primers in a 30-μl reaction mixture. cDNA (1 μl) was used as the template for real-time reaction mixtures containing primer sets and iQ SYBR green Supermix (Bio-Rad). Primers FRE-S-RT-2 and FRE-A-RT-2 were used to amplify *C. neoformans FRE3*, and the products were compared to those of equivalent reactions with primers ACT1-1200S and ACT1-1455A for normalization. qPCR data were analyzed with Bio-Rad iQ5 software, and results are presented as normalized expression ($\Delta\Delta C_T$) for the microarray validation studies.

Sequence data mining and analysis. *C. neoformans* and *S. cerevisiae* sequence data were retrieved from the NCBI Broad Institute website and the *Saccharomyces* Genome Database, respectively. For the analysis of cryptococcal and yeast Fe reductase-related motifs, sequences were retrieved by BLASTp searches with yeast *FRE*1-8 and *C. neoformans* CNAG_06524 as the query sequences. The full protein sequences were aligned with MUSCLE (57), and motifs were manually extracted and aligned (see Fig. S1 in the supplemental material). A phylogenetic analysis of the conserved motifs (Fig. 3B) was performed with the heuristic parsimony algorithm of PAUP 4b10 (58). To evaluate support for the groups in the tree, 500 nonparametric bootstrap replicates were analyzed. PAUP returned 500 equally parsimonious trees for which the 50% majority rule consensus is shown. All of the variation among the equally parsimonious trees occurred within these collapsed groups, so the branches shown in Fig. 2 were found in all 500 trees. Bootstrap support values of >70% were considered significant. Predicted transmembrane regions were identified by two prediction programs, MEMSAT (59) and Phobium (60).

Construction of *FRE3* RNAi and *FRE3*-overexpressing *C. neoformans* strains. The cryptococcal shuttle vector pORA-KUTAP, containing the *URA5* transformation marker, was used to effect RNAi suppression of *C. neoformans FRE3* as described by Panepinto et al. (65), modified by the substitution of a 500-bp fragment of intron I of *LAC1* for the intervening region between the sense and antisense strands. Briefly, to construct the *FRE3* RNAi strain, pORA-KUTAP, containing the EF-1α terminator sequence, was digested with EcoRI and ligated simultaneously to a mixture of an XhoI-digested PCR-amplified *LAC1* intron fragment from H99 (with primers IntronS-Xho and IntronA-Xho; see Table S1 in the supplemental material) and a second XhoI- and EcoRI-digested, PCR-amplified fragment of the *C. neoformans FRE2* open reading frame (with primers Fre-KD-S-RI and Fre-KD-A-XhoI) to produce pFre3-RNAi. To construct the *FRE3*-overexpressing strain, pORA-KUTAP was digested with EcoRI and ligated with amplified *FRE3* fragments from cDNA with primers FRE-2-RI and FRE-A-RI to produce pFre3-OEx. The plasmids were recovered, their sequences were verified, and they were linearized with SceI and transformed into *C. neoformans* H99 *Mat***a** *ura5* cells by electroporation by standard methods (56). An H99 *Mat***a** *ura5* strain transformed with plasmid pORA-KUTAP without the RNAi construct served as a control for *URA5* expression for *in vivo* studies. Transformants were selected by equivalent copy number demonstrated by uncut Southern analysis as described previously (65), and expression in all transformants was verified to be at least more than five times the endogenous expression of the precursor strain by qPCR (see Table S1 for the sequences of the primers used). All of the *C. neoformans* strains recovered from nonselective medium or animals were tested for growth on YPD and ASN minimal medium to verify that >90% of them had retained the plasmids indicated.

Iron reductase assay. Iron reductase activity was assayed by the method of Nyhus and Jacobson (35). Briefly, cells were grown overnight in ASN medium with 2% glucose and then transferred to limited-iron medium (LIM). At the indicated time of induction in LIM, 1×10^6-cell aliquots were removed, mixed with ferric hydroxyethylethylenetriacetic acid and bathophenanthrolinedisulfonic acid at 1 mM each, and incubated for 1 h prior to the reading of A_{535} as previously described (61). For copper reductase assays, cells were prepared as described above but assays were conducted mixed with $CuSO_4$ and bathocuproine disulfonate (BCDS) at 1 mM each and copper reductase activity was measured by Cu(I)-BCDS complex formation at A_{478}.

Phagocytosis assay. Phagocytosis and fungal killing assays were conducted with J774.16 cells by the method of Shapiro et al. (62) Approximately 5×10^4 J774.16 macrophage-like cells/well were plated in complete Dulbecco's modified Eagle medium (DMEM) and incubated overnight at 37°C in a 5% CO_2 atmosphere. Cells were continuously kept under the stimulation of recombinant murine gamma interferon (IFN-γ) at 100 U ml^{-1}. *C. neoformans* H99 cells grown for 48 h in YPD were washed three times with phosphate-buffered saline (PBS) and resuspended in DMEM supplemented with 20% mouse serum (Pel-Freez Biologicals, Rogers, AR), incubated for 20 min in 40% serum, and subsequently added to a macrophage monolayer at a 1:5 macrophage-to-yeast ratio. Unopsonized yeast cells resuspended in DMEM (lacking mouse serum) were used as a control. After a 1-h incubation at 37°C, the macrophage monolayer was washed three times with PBS and stained with FUN-1 in distilled water. The phagocytosis index was determined by microscopic examination of the number of fungal cells ingested or adherent divided by the total number of macrophages. At least 300 macrophages were analyzed for each condition, and the results of three independent experiments are shown.

Fungal killing by J774.16 cells. The method of Wormley and Perfect (66) was used to assay fungal killing by J774.16 cells. Briefly, 1×10^5 cells of J774.16 (obtained from the American Type Culture Collection) in a volume of 50 μl per well was added to flat-bottom 96-well plates, supplemented with IFN-γ (100 U/ml) and lipopolysaccharide (0.6 μg/ml), and incubated at 37°C with 5% CO_2 for 12 to 18 h. Overnight cultures of the *C. neoformans* strains indicated were washed at 5,000 $\times$ *g* three times for 5 min, yeast pellets were suspended in 10 ml of DMEM, and the numbers of viable yeast cells were quantified. Yeast cells were suspended in DMEM containing monoclonal antibody 18B7 (1 μg/ml) at 10^6/ml and incubated for 1 h at 37°C. Yeast cells were added (10^5 cells/100 μl) to macrophages in a 96-well tissue culture plate, incubated at 37°C at 5% CO_2 for 1 h, and then washed three times with sterile PBS to remove extracellular yeast. After the removal of extracellular yeast, 200 μl of DMEM was added to each well and the plate was again incubated at 37°C for 8 h. A 100-μl volume of 0.05% SDS was added to each well to lyse monocytes and release phagocytized yeast cells. The wells were washed three times with sterile water, the washes were pooled and serially diluted, and the CFU counts in portions of the final dilution (100 μl to 1.0 ml) were quantified. Fungal survival was expressed as the CFU count at 8 h as a percentage of that at the 1-h time point.

Multilocus sequence alignment. DNA was isolated by standard methods from the *C. neoformans* strains indicated. PCR amplification of multilocus sequence typing (MLST) allelic regions for the highly conserved regions of six genes (*CAP59*, *GDP1*, *LAC1*, *PLB1*, *SOD1*, and *URA5*) was performed with PfuUltra HotStart DNA polymerase (Agilent Technologies) according to the *C. neoformans* MLST consortium (28). The primer sequences, consensus MLST loci, and lengths of the trimmed sequence files used were from the Pathogenic Fungi MLST Database (http://mlst.mycologylab.org/defaultinfo.aspx?Page=MLSTconsensustable). PCR products were run on a 2% agarose gel to confirm product size prior to DNA sequencing. Trimmed MLST sequences were concatenated, resulting in the inclusion of 3,271 to 3,463 characters for alignment and phylogenetic analysis with ClustalW (63, 64). Distances included for the unrooted tree were calculated by using ClustalW phylogeny. Distance values show the number of substitutions as a proportion of the length of the alignment, excluding gaps.

Determination of ploidy by flow cytometry. Cells were stained with propidium iodide and analyzed for fluorescence intensity by flow cytom-

etry by the method of Lin et al. (67). Serotype A strain H99 was used as a haploid reference strain. Environmental strains were grown in YPD broth overnight at 30°C. Cells were harvested at 10^7/ml, washed twice in distilled water, and fixed in 70% ethanol overnight at 4°C. Cells were washed twice with distilled water, stained with propidium iodide (10 μg/ml) in 15 mM sodium phosphate buffer containing RNase (1 mg/ml), and incubated at 37°C for 2 h. Stained cells were diluted in Tris-HCl (1 M pH 8.0), and 10^4 cells were counted by flow cytometry (BD LSRFortessa) at 488 nm.

Statistics. The capsule radius was measured in India ink experiments by using 10 cells of each strain, and means were compared by ANOVA with Tukey's *post hoc* test. Errors were expressed as the standard errors of the means (SEMs). The statistical significance of differences in mouse survival times was assessed by Kruskal-Wallis analysis (ANOVA on ranks). Comparisons of growth doubling times, *FRE3* expression levels, ferric reductase activities, phagocytic indexes, and fungal survival times were performed by a nonparametric *t* test with Welch's correction. Plots, curve fits, Pearson or Spearman correlations (*r*), and statistical analyses were performed with GraphPad Prism version 5.0a (GraphPad Software, San Diego, CA).

SUPPLEMENTAL MATERIAL

Supplemental material for this article may be found at http://mbio.asm.org/lookup/suppl/doi:10.1128/mBio.00941-14/-/DCSupplemental.

Figure S1, DOCX file, 0.1 MB.
Figure S2, DOCX file, 0.2 MB.
Figure S3, DOCX file, 4.3 MB.
Figure S4, DOCX file, 0.6 MB.
Figure S5, DOCX file, 0.1 MB.
Table S1, DOCX file, 0.1 MB.

ACKNOWLEDGMENTS

This research was supported by the Intramural Research Program of the NIH, NIAID.

We appreciate the bioinformatic technical expertise of K. Wollenberg, Peter Larsen, and F. Otaizo-Carrasquero; P. Gardina for data analysis; and helpful discussions by B. Boeckmann.

REFERENCES

1. **Ebert D.** 1998. Experimental evolution of parasites. Science **282:**1432–1435. http://dx.doi.org/10.1126/science.282.5393.1432.
2. **Steenbergen JN, Shuman HA, Casadevall A.** 2001. *Cryptococcus neoformans* interactions with amoebae suggest an explanation for its virulence and intracellular pathogenic strategy in macrophages. Proc. Natl. Acad. Sci. U. S. A. **98:**15245–15250. http://dx.doi.org/10.1073/pnas.261418798.
3. **Warpeha KM, Park YD, Williamson PR.** 2013. Susceptibility of intact germinating *Arabidopsis thaliana* to the human fungal pathogen *Cryptococcus*. Appl. Environ. Microbiol. **79:**2979–2988. http://dx.doi.org/10.1128/AEM.03697-12.
4. **Park BJ, Wannemuehler KA, Marston BJ, Govender N, Pappas PG, Chiller TM.** 2009. Estimation of the current global burden of cryptococcal meningitis among persons living with HIV/AIDS. AIDS **23:**525–530. http://dx.doi.org/10.1097/QAD.0b013e328322ffac.
5. **Pyrgos V, Seitz AE, Steiner CA, Prevots DR, Williamson PR.** 2013. Epidemiology of cryptococcal meningitis in the US: 1997–2009. PLoS One 8:e56269.http://dx.doi.org/10.1371/journal.pone.0056269.
6. **Chen LC, Goldman DL, Doering TL, Pirofski La, Casadevall A.** 1999. Antibody response to *Cryptococcus neoformans* proteins in rodents and humans. Infect. Immun. **67:**2218–2224.
7. **Goldman DL, Khine H, Abadi J, Lindenberg DJ, Pirofski La, Niang R, Casadevall A.** 2001. Serologic evidence for *Cryptococcus neoformans* infection in early childhood. Pediatrics **107:**E66. http://dx.doi.org/10.1542/peds.107.5.e66.
8. **Garcia-Hermoso D, Janbon G, Dromer F.** 1999. Epidemiological evidence for dormant *Cryptococcus neoformans* infection. J. Clin. Microbiol. **37:**3204–3209.
9. **McClelland EE, Adler FR, Granger DL, Potts WK.** 2004. Major histocompatibility complex controls the trajectory but not host-specific adaptation during virulence evolution of the pathogenic fungus *Cryptococcus neoformans*. Proc. Biol. Sci. **271:**1557–1564. http://dx.doi.org/10.1098/rspb.2004.2736.
10. **McClelland EE, Granger DL, Potts WK.** 2003. Major histocompatibility complex-dependent susceptibility to *Cryptococcus neoformans* in mice. Infect. Immun. **71:**4815–4817. http://dx.doi.org/10.1128/IAI.71.8.4815-4817.2003.
11. **McClelland EE, Perrine WT, Potts WK, Casadevall A.** 2005. Relationship of virulence factor expression to evolved virulence in mouse-passaged *Cryptococcus neoformans* lines. Infect. Immun. **73:**7047–7050. http://dx.doi.org/10.1128/IAI.73.10.7047-7050.2005.
12. **Pedroso RS, Ferreira JC, Lavrador MA, Maffei CM, Candido RC.** 2009. Evaluation of the experimental inoculation of Cryptococcus albidus and Cryptococcus laurentii in normal mice: virulence factors and molecular profile before and after animal passage. Mycopathologia **168:**59–72. http://dx.doi.org/10.1007/s11046-009-9202-z.
13. **Fries BC, Casadevall A.** 1998. Serial isolates of *Cryptococcus neoformans* from patients with AIDS differ in virulence for mice. J. Infect. Dis. **178:**1761–1766. http://dx.doi.org/10.1086/314521.
14. **Schiappa D, Gueyikian A, Kakar S, Alspaugh JA, Perfect JR, Williamson PR.** 2002. An auxotrophic pigmented *Cryptococcus neoformans* strain causing infection of the bone marrow. Med. Mycol. **40:**1–5. http://dx.doi.org/10.1080/714031078.
15. **Pedroso RS, Lavrador MA, Ferreira JC, Candido RC, Maffei CM.** 2010. *Cryptococcus neoformans* var. grubii—pathogenicity of environmental isolates correlated to virulence factors, susceptibility to fluconazole and molecular profile. Mem. Inst. Oswaldo Cruz **105:**993–1000. http://dx.doi.org/10.1590/S0074-02762010000800008.
16. **Steenbergen JN, Nosanchuk JD, Malliaris SD, Casadevall A.** 2003. *Cryptococcus neoformans* virulence is enhanced after growth in the genetically malleable host *Dictyostelium discoideum*. Infect. Immun. **71:**4862–4872. http://dx.doi.org/10.1128/IAI.71.9.4862-4872.2003.
17. **Currie B, Sanati H, Ibrahim AS, Edwards JE, Jr, Casadevall A, Ghannoum MA.** 1995. Sterol compositions and susceptibilities to amphotericin B of environmental *Cryptococcus neoformans* isolates are changed by murine passage. Antimicrob. Agents Chemother. **39:**1934–1937. http://dx.doi.org/10.1128/AAC.39.9.1934.
18. **Waterman SR, Hacham M, Hu G, Zhu X, Park YD, Shin S, Panepinto J, Valyi-Nagy T, Beam C, Husain S, Singh N, Williamson PR.** 2007. Role of a *CUF1-CTR4* copper regulatory axis in the virulence of *Cryptococcus neoformans*. J. Clin. Invest. **117:**794–802. http://dx.doi.org/10.1172/JCI30006.
19. **Magditch DA, Liu TB, Xue C, Idnurm A.** 2012. DNA mutations mediate microevolution between host-adapted forms of the pathogenic fungus *Cryptococcus neoformans*. PLoS Pathog. **8:**e1002936. http://dx.doi.org/10.1371/journal.ppat.1002936.
20. **Bunting LA, Neilson JB, Bulmer GS.** 1979. *Cryptococcus neoformans*: gastronomic delight of a soil ameba. Sabouraudia **17:**225–232. http://dx.doi.org/10.1080/00362177985380341.
21. **Neilson JB, Ivey MH, Bulmer GS.** 1978. *Cryptococcus neoformans*: pseudohyphal forms surviving culture with *Acanthamoeba polyphaga*. Infect. Immun. **20:**262–266.
22. **Ruiz A, Neilson JB, Bulmer GS.** 1982. Control of *Cryptococcus neoformans* in nature by biotic factors. Sabouraudia **20:**21–29. http://dx.doi.org/10.1080/00362178285380051.
23. **Georgatsou E, Alexandraki D.** 1999. Regulated expression of the *Saccharomyces cerevisiae* Fre1p/Fre2p Fe/Cu reductase related genes. Yeast **15:**573–584. http://dx.doi.org/10.1002/(SICI)1097-0061(199905)15:7<573::AID-YEA404>3.0.CO;2-7.
24. **Askwith CC, de Silva D, Kaplan J.** 1996. Molecular biology of iron acquisition in *Saccharomyces cerevisiae*. Mol. Microbiol. **20:**27–34. http://dx.doi.org/10.1111/j.1365-2958.1996.tb02485.x.
25. **Dancis A, Yuan DS, Haile D, Askwith C, Eide D, Moehle C, Kaplan J, Klausner RD.** 1994. Molecular characterization of a copper transport protein in *S. cerevisiae*: an unexpected role for copper in iron transport. Cell **76:**393–402. http://dx.doi.org/10.1016/0092-8674(94)90345-X.
26. **Caza M, Kronstad JW.** 2013. Shared and distinct mechanisms of iron acquisition by bacterial and fungal pathogens of humans. Front. Cell. Infect. Microbiol. **3:**80. http://dx.doi.org/10.3389/fcimb.2013.00080.
27. **Jennings A, Bennett JE, Young V.** 1968. Identification of *Cryptococcus neoformans* in a routine clinical laboratory. Mycopathol. Mycol. Appl. **35:**256–264. http://dx.doi.org/10.1007/BF02050740.
28. **Meyer W, Aanensen DM, Boekhout T, Cogliati M, Diaz MR, Esposto MC, Fisher M, Gilgado F, Hagen F, Kaocharoen S, Litvintseva AP,**

Mitchell TG, Simwami SP, Trilles L, Viviani MA, Kwon-Chung J. 2009. Consensus multi-locus sequence typing scheme for *Cryptococcus neoformans* and *Cryptococcus gattii*. Med. Mycol. **47:**561–570. http://dx.doi.org/10.1080/13693780902953886.

29. **Franzot SP, Mukherjee J, Cherniak R, Chen LC, Hamdan JS, Casadevall A.** 1998. Microevolution of a standard strain of *Cryptococcus neoformans* resulting in differences in virulence and other phenotypes. Infect. Immun. **66:**89–97.
30. **Williamson PR.** 1994. Biochemical and molecular characterization of the diphenol oxidase of *Cryptococcus neoformans*: identification as a laccase. J. Bacteriol. **176:**656–664.
31. **Hu G, Hacham M, Waterman SR, Panepinto J, Shin S, Liu X, Gibbons J, Valyi-Nagy T, Obara K, Jaffe HA, Ohsumi Y, Williamson PR.** 2008. PI3K signaling of autophagy is required for starvation tolerance and virulence of *Cryptococcus neoformans*. J. Clin. Invest. **118:**1186–1197. http://dx.doi.org/10.1172/JCI32053.
32. **Price MS, Betancourt-Quiroz M, Price JL, Toffaletti DL, Vora H, Hu G, Kronstad JW, Perfect JR.** 2011. *Cryptococcus neoformans* requires a functional glycolytic pathway for disease but not persistence in the host. mBio **2:**e00103-11. http://dx.doi.org/10.1128/mBio.00103-11.
33. **Finegold AA, Shatwell KP, Segal AW, Klausner RD, Dancis A.** 1996. Intramembrane bis-heme motif for transmembrane electron transport conserved in a yeast iron reductase and the human NADPH oxidase. J. Biol. Chem. **271:**31021–31024. http://dx.doi.org/10.1074/jbc.271.49.31021.
34. **Zhang X, Krause KH, Xenarios I, Soldati T, Boeckmann B.** 2013. Evolution of the ferric reductase domain (FRD) superfamily: modularity, functional diversification, and signature motifs. PLoS One **8:**e58126. http://dx.doi.org/10.1371/journal.pone.0058126.
35. **Nyhus KJ, Jacobson ES.** 1999. Genetic and physiologic characterization of ferric-cupric reductase constitutive mutants of *Cryptococcus neoformans*. Infect. Immun. **67:**2357–2365.
36. **Georgatsou E, Mavrogiannis LA, Fragiadakis GS, Alexandraki D.** 1997. The yeast Fre1p/Fre2p cupric reductases facilitate copper uptake and are regulated by the copper-modulated Mac1p activator. J. Biol. Chem. **272:**13786–13792. http://dx.doi.org/10.1074/jbc.272.21.13786.
37. **Feldmesser M, Kress Y, Novikoff P, Casadevall A.** 2000. *Cryptococcus neoformans* is a facultative intracellular pathogen in murine pulmonary infection. Infect. Immun. **68:**4225–4237. http://dx.doi.org/10.1128/IAI.68.7.4225-4237.2000.
38. **Fries BC, Chen F, Currie BP, Casadevall A.** 1996. Karyotype instability in *Cryptococcus neoformans* infection. J. Clin. Microbiol. **34:**1531–1534.
39. **Crichton RR, Pierre JL.** 2001. Old iron, young copper: from Mars to Venus. Biometals 14:99–112. PubMed. doi:10.1023/A:1016710810701. PubMed.
40. **Kosman DJ.** 2003. Molecular mechanisms of iron uptake in fungi. Mol. Microbiol. **47:**1185–1197. http://dx.doi.org/10.1046/j.1365-2958.2003.03368.x.
41. **Silva MG, Schrank A, Bailao EF, Bailao AM, Borges CL, Staats CC, Parente JA, Pereira M, Salem-Izacc SM, Mendes-Giannini MJ, Oliveira RM, Silva LK, Nosanchuk JD, Vainstein MH, de Almeida Soares CM.** 2011. The homeostasis of iron, copper, and zinc in *Paracoccidioides brasiliensis*, *Cryptococcus neoformans* var. grubii, and *Cryptococcus gattii*: a comparative analysis. Front. Microbiol. **2:**49. http://dx.doi.org/10.3389/fmicb.2011.00049.
42. **Shi X, Stoj C, Romeo A, Kosman DJ, Zhu Z.** 2003. Fre1p Cu^{2+} reduction and Fet3p Cu^{1+} oxidation modulate copper toxicity in *Saccharomyces cerevisiae*. J. Biol. Chem. **278:**50309–50315. http://dx.doi.org/10.1074/jbc.M307019200.
43. **Hassett R, Kosman DJ.** 1995. Evidence for Cu(II) reduction as a component of copper uptake by Saccharomyces cerevisiae. J. Biol. Chem. **270:**128–134. http://dx.doi.org/10.1074/jbc.270.1.128.
44. **Adler A, Park YD, Larsen P, Nagarajan V, Wollenberg K, Qiu J, Myers TG, Williamson PR.** 2011. A novel specificity protein 1 (SP1)-like gene regulating protein kinase C-1 (Pkc1)-dependent cell wall integrity and virulence factors in *Cryptococcus neoformans*. J. Biol. Chem. **286:**20977–20990. http://dx.doi.org/10.1074/jbc.M111.230268.
45. **Jung WH, Saikia S, Hu G, Wang J, Fung CK, D'Souza C, White R, Kronstad JW.** 2010. HapX positively and negatively regulates the transcriptional response to iron deprivation in *Cryptococcus neoformans*. PLoS Pathog. **6:**e1001209. http://dx.doi.org/10.1371/journal.ppat.1001209.
46. **Polacheck I, Hearing VJ, Kwon-Chung KJ.** 1982. Biochemical studies of phenoloxidase and utilization of catecholamines in *Cryptococcus neoformans*. J. Bacteriol. **150:**1212–1220.
47. **Jung WH, Kronstad JW.** 2011. The iron-responsive, GATA-type transcription factor Cir1 influences mating in *Cryptococcus neoformans*. Mol. Cells **31:**73–77. http://dx.doi.org/10.1007/s10059-011-0011-0.
48. **Liu L, Tewari RP, Williamson PR.** 1999. Laccase protects *Cryptococcus neoformans* from antifungal activity of alveolar macrophages. Infect. Immun. **67:**6034–6039.
49. **Ma H, Hagen F, Stekel DJ, Johnston SA, Sionov E, Falk R, Polacheck I, Boekhout T, May RC.** 2009. The fatal fungal outbreak on Vancouver Island is characterized by enhanced intracellular parasitism driven by mitochondrial regulation. Proc. Natl. Acad. Sci. U. S. A. **106:**12980–12985. http://dx.doi.org/10.1073/pnas.0902963106.
50. **Gutierrez MC, Brisse S, Brosch R, Fabre M, Omaïs B, Marmiesse M, Supply P, Vincent V.** 2005. Ancient origin and gene mosaicism of the progenitor of Mycobacterium tuberculosis. PLoS Pathog. **1:**e5. http://dx.doi.org/10.1371/journal.ppat.0010005.
51. **Fan W, Kraus PR, Boily MJ, Heitman J.** 2005. *Cryptococcus neoformans* gene expression during murine macrophage infection. Eukaryot. Cell **4:**1420–1433. http://dx.doi.org/10.1128/EC.4.8.1420-1433.2005.
52. **Chen Y, Toffaletti DL, Tenor JL, Litvintseva AP, Fang C, Mitchell TG, McDonald TR, Nielsen K, Boulware DR, Bicanic T, Perfect JR.** 2014. The *Cryptococcus neoformans* transcriptome at the site of human meningitis. mBio **5:**e01087-13. http://dx.doi.org/10.1128/mBio.01087-13.
53. **Wilson DE, Bennett JE, Bailey JW.** 1968. Serologic grouping of *Cryptococcus neoformans*. Proc. Soc. Exp. Biol. Med. **127:**820–823. http://dx.doi.org/10.3181/00379727-127-32812.
54. **Varma A, Edman JC, Kwon-Chung KJ.** 1992. Molecular and genetic analysis of *URA5* transformants of *Cryptococcus neoformans*. Infect. Immun. **60:**1101–1108.
55. **Nyhus KJ, Wilborn AT, Jacobson ES.** 1997. Ferric iron reduction by *Cryptococcus neoformans*. Infect. Immun. **65:**434–438.
56. **Erickson T, Liu L, Gueyikian A, Zhu X, Gibbons J, Williamson PR.** 2001. Multiple virulence factors of *Cryptococcus neoformans* are dependent on *VPH1*. Mol. Microbiol. **42:**1121–1131. http://dx.doi.org/10.1046/j.1365-2958.2001.02712.x.
57. **Edgar RC.** 2004. MUSCLE: multiple sequence alignment with high accuracy and high throughput. Nucleic Acids Res. **32:**1792–1797. http://dx.doi.org/10.1093/nar/gkh340.
58. **Swofford D.** 2003. PAUP, phylogenetic analysis using parsimony. Sinauer Associates, Sunderland, MA.
59. **Jones DT, Taylor WR, Thornton JM.** 1994. A model recognition approach to the prediction of all-helical membrane protein structure and topology. Biochemistry **33:**3038–3049. http://dx.doi.org/10.1021/bi00176a037.
60. **Käll L, Krogh A, Sonnhammer EL.** 2004. A combined transmembrane topology and signal peptide prediction method. J. Mol. Biol. **338:**1027–1036. http://dx.doi.org/10.1016/j.jmb.2004.03.016.
61. **Cox CD.** 1994. Deferration of laboratory media and assays for ferric and ferrous ions. Methods Enzymol. **235:**315–329. http://dx.doi.org/10.1016/0076-6879(94)35150-3.
62. **Shapiro S, Beenhouwer DO, Feldmesser M, Taborda C, Carroll MC, Casadevall A, Scharff MD.** 2002. Immunoglobulin G monoclonal antibodies to *Cryptococcus neoformans* protect mice deficient in complement component C3. Infect. Immun. **70:**2598–2604. http://dx.doi.org/10.1128/IAI.70.5.2598-2604.2002.
63. **Goujon M, McWilliam H, Li W, Valentin F, Squizzato S, Paern J, Lopez R.** 2010. A new bioinformatics analysis tools framework at EMBL-EBI. Nucleic Acids Res. **38:**W695–W699. http://dx.doi.org/10.1093/nar/gkq313.
64. **Larkin MA, Blackshields G, Brown NP, Chenna R, McGettigan PA, McWilliam H, Valentin F, Wallace IM, Wilm A, Lopez R, Thompson JD, Gibson TJ, Higgins DG.** 2007. ClustalW2 and ClustalX version 2. Bioinformatics **23:**2947–2948. http://dx.doi.org/10.1093/bioinformatics/btm404.
65. **Panepinto J, Komperda K, Frases S, Park YD, Djordjevic JT, Casadevall A, Williamson PR.** 2009. Sec6-dependent sorting of fungal extracellular exosomes and laccase of *Cryptococcus neoformans*. Mol. Microbiol. **71**(5):1165–1176.
66. **Wormley FL, Jr, Perfect JR.** 2005. Immunology of infection caused by *Cryptococcus neoformans*. Methods Mol. Med. **118:**193–198.
67. **Lin X, Hull CM, Heitman J.** 2005. Sexual reproduction between partners of the same mating type in *Cryptococcus neoformans*. Nature **434:**1017–1021.